

WHITE PAPER

Validation of an Off-the-Shelf, Diet-Induced NASH Mouse Model using Digital Whole Slide Scanning of Liver Tissue and Artificial Intelligence-Enabled, Quantitative Histopathological Analysis

Daniel Schroen, PhD, Commercial Lead, R&D, Reveal Biosciences (corresponding author, dschroen@revealbio.com)

Susan Kelly, HTL(ASCP)QIHC, Histology Group Lead, Reveal Biosciences

Manindra Singh, PhD, Scientist I, Explora BioLabs

Brandy Wilkinson, PhD, Director Breeding and Research, Explora BioLabs

Christopher Coley, Marketing Development Manager, Digital Pathology, EpreDia

Sara Becker Catania, PhD, Associate Director, Product Development, Reveal Biosciences

SUMMARY

Non-alcoholic fatty liver disease (NAFLD) and non-alcoholic steatohepatitis (NASH) are common chronic liver disorders resulting in lipid accumulation in the liver, inflammation, hepatocyte damage, and fibrotic scarring, all of which impact organ function. With the lack of approved therapies for NASH patients, and considerable inter-pathologist variability in the scoring and semi-quantitative assessment of the pathology used in their diagnoses, much focus and effort is being placed in the development of rodent models, the assessment of individual disease features in these models, and understanding the effect of therapeutics on the disease process. The study described in this paper is the result of a unique collaboration between several companies with combined goals of providing the NASH research community with a time-efficient, flexible, off-the-shelf diet-induced mouse NASH B6 Model (Taconic Biosciences, Inc.) that can be utilized in directed research studies for therapeutic drug development (Explora BioLabs). The results were digitally scanned using a 3DHISTECH PANNORAMIC™ series scanner (EpreDia) and validated with imageDx NASH, a digital assay platform featuring machine and deep learning models to quantify steatosis, inflammation, hepatocellular ballooning, and fibrosis (Reveal Biosciences, Inc). AI-generated quantitative results were compared with qualitative NAS scores provided by a board-certified veterinary pathologist to evaluate grade and fibrosis stage. The AI-based digital analysis results of the treated and untreated diet-induced NASH B6 model correlated with the CRN scores recorded by the experienced veterinary pathologist. Importantly, the quantitative data also demonstrated measurement of more granular pathologic changes. These subtle - but likely significant - pathologic changes are not currently well-captured by the standard scoring system, and underscore the need for and the utility for sensitive and reproducible quantitative analysis.

INTRODUCTION

NAFLD/NASH

Non-alcoholic fatty liver disease (NAFLD) is one of the most common causes of chronic liver disease and results in an accumulation of fat in the liver, often with few or no symptoms. NAFLD can progress to a more pathologically significant form of NAFLD known as non-alcoholic steatohepatitis (NASH), characterized by hepatitis (inflammation) and hepatocellular ballooning (cell injury), which can lead to excessive fibrosis and scarring. NASH has the potential to progress to more extensive pathologic features including portal hypertension, cirrhosis and hepatocellular carcinoma, resulting in impaired liver function that often requires liver transplantation as treatment. The incidence of NAFLD/NASH has increased in the last ten years and is growing, at least partially due to increasing incidence of risk factors such as type 2 diabetes, insulin resistance,

metabolic syndrome, and patients with high blood pressure, cholesterol, lipids and triglycerides.

Mouse models in NASH research

At present, the US Food and Drug Administration (FDA) has yet to approve any therapies for the treatment of NASH. However, with the increased incidence of NAFLD and NASH, the biopharmaceutical industry has expressed active interest in developing drugs and treatments for NASH, with initial studies requiring the use of animal models. Although multiple mouse models of NAFLD/NASH exist, they have been limited by the lack of well-validated animal models that accurately mimic the human disease's multifactorial features. The ideal experimental mouse model would closely replicate human macrovesicular steatosis, hepatocyte ballooning,

and fibrosis, and respond in a fashion similar to how patients would react to therapeutic interventions. A number of drug candidates, spread throughout phase I-III clinical trials, include inhibitors, receptor agonists, and antibodies, used singly or in combination. Their targets include insulin resistance, gluconeogenesis, lipogenesis and lipid transport, all targeting steatosis and reduction of lipid accumulation. At more severe stages of disease, therapeutics are directed towards apoptosis, oxidative stress and inflammation, all hallmark features of steatohepatitis. At the most progressive stage of disease, therapeutics address pathways that result in excessive deposition of extracellular matrix (ECM) components, with the aim to thwart or reverse cirrhosis. Animal models that successfully recapitulate these stages of the human disease continuum provide the best opportunity for therapeutic development.

As a readout for therapeutic treatment, NASH/NAFLD mouse models are either induced by diet (obesogenic, nutrient deficient, or chemically induced), and/or are genetically predisposed to develop the phenotypic characteristics of NASH. However, many of these models do not successfully establish all features of the human disease. Diet-induced models such as the Taconic Diet Induced NASH B6 develop the NAFLD/NASH phenotype following extended ingestion of a high fat, high sugar, high cholesterol diet. One limitation of current diet-induced models is the amount of time it takes to evolve features of NAFLD/NASH. With the recent availability of off-the-shelf NASH B6 mice (Taconic Biosciences) already on a modified Amylin Liver NASH (NASH) diet, researchers can reduce the time to development of steatosis, inflammation, and fibrosis with a consistent and cost-effective approach. In this study, NASH B6 mice are treated with two different therapeutic candidates. Elafibranor, a dual peroxisome proliferator-activated receptor (PPAR) agonist, targets PPARalpha and PPARdelta, primarily affecting hepatocyte ballooning and inflammation (Ratziu et al. 2017). Obeticholic acid (OCA), a semi-synthetic bile acid analog, functions as a farnesoid X receptor agonist, thereby decreasing the amount of bile in the liver and improving steatosis, inflammation, and fibrosis (Makri et al. 2016).

Analysis of NASH features

The increasing incidence of NASH, and its associated potential for more serious liver disease, has compelled development of new methods to detect NASH earlier, to differentiate NAFLD from NASH, and to ensure reliable, consistent measurements of the disease process in

preclinical animal studies. In addition to the challenges associated with generating validated mouse models, one must also ensure consistent and unbiased measurements of pathologic features. Along with monitoring body weight and blood analytes, liver biopsy and associated histologic analysis remains the gold standard for diagnosing NASH/NAFLD. Semi-quantitative reporting of steatosis, inflammation, ballooning, and fibrosis is typically done using the NASH CRN grading and staging system (Kleiner et al. 2005). Although biopsy and subsequent histologic staining of sections is quite routine, the analysis and stage designation for each NAFLD/NASH feature can be markedly subjective. Inter-pathologist concordance studies indicate low Kappa Scores for different histologic features, with published data ranging from 0.45-0.84 (Kleiner 2005), 0.41-0.61 (Bedossa 2014), and 0.46-0.77 (Kleiner 2019). The NAFLD activity score (NAS), widely used to assess pathology in biopsies, is an 8-point scale measuring steatosis, ballooning, and inflammation. However, subjectivity, its semi quantitative nature, and high interobserver variability limit the NAFLD activity score, which has not been shown to have prognostic value. To address subjectivity in liver pathology staging, Reveal Biosciences has developed a novel digital assay providing quantitative analysis for each of the pathologic features of NAFLD/NASH. This approach leverages both machine learning (ML) and deep learning to provide a more quantitative and less-subjective approach to measure and stage liver pathology.

ImageDx™ NASH Analysis

Reveal Biosciences launched the imageDx™ NASH digital assay platform in 2019, a project developed in close collaboration with a team of leading US liver pathologists to support both the pre-clinical and research sector, as well as to provide support for NASH clinical pathologists. As a cloud-based decision support tool for quantitative NASH data, imageDx greatly enhances project accuracy, reproducibility and scale. This platform provides image hosting with broad geographical access, facilitating collaboration, image sharing, annotation and analysis. Based on precise, consistent machine and deep learning, imageDx yields accurate quantification across samples, with AI-based NASH models trained from thousands of image patches. In the imageDx workflow, tissue samples are processed at Reveal Bio or any quality histopathology lab, after which whole slide images are generated and uploaded to the imageDx cloud for analysis. Custom analysis and continuous, quantitative results are then produced for review. Built-in

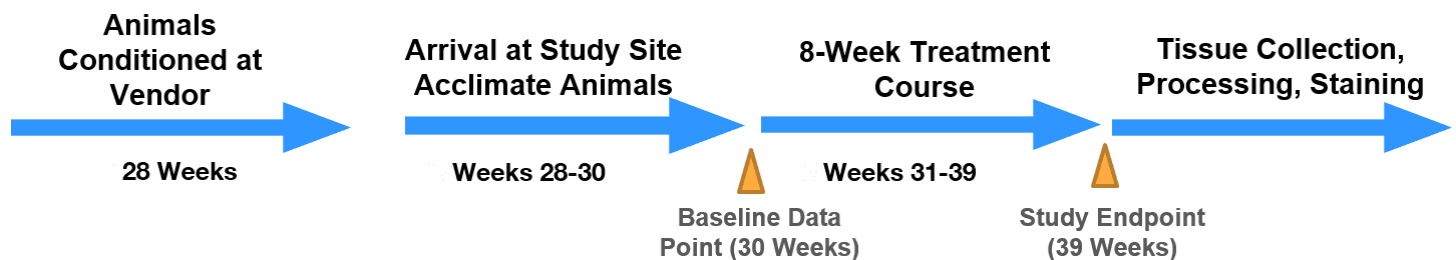
quality controls automatically detect and exclude tissue artifacts, folds, tears, out-of-focus regions, and slide debris that may otherwise impact data quality.

While the most applicable mouse NASH models replicate pathology seen in human NASH liver, some differences are inherent to mouse tissues. Therefore, the imageDx™ NASH digital assay was developed to specifically address species differences. Individual AI scoring algorithms have been developed and validated specifically for rodent and human liver to generate accurate analysis. For staging of rodent NASH liver

samples, the imageDx™ NASH digital assay offers a non-subjective, validated alternative or addition to pathologist review of stained liver samples. The analysis uses hematoxylin and eosin (H&E), Masson’s trichrome (MTC) or Picrosirius red (PSR)-stained slides for the analysis of steatosis, ballooning, inflammation, fibrosis and the presence of Mallory bodies. In this study, the quantitative results from the imageDx™ NASH analysis were run in parallel and compared to results from a board-certified veterinary pathologist.

MATERIALS AND METHODS

Starting at 6 weeks of age, thirty (30) C57BL/6NTac male mice (Taconic Biosciences, Inc., Rensselaer, NY, USA) were conditioned for 28 weeks (at the vendor) on high-fat, modified Amylin liver NASH rodent diet D09100310i (Research Diets, Inc., New Brunswick, NJ USA), containing 40 kcal% Fat (Palm Oil), 20 kcal% Fructose and 2% Cholesterol. Following arrival at the study site (Explora BioLabs) during week 28 of diet conditioning, animals were acclimated for 2 more weeks until week 30 at which time a group of animals was sacrificed for baseline data and another group was selected for an 8-week treatment beginning in week 31 with the animals sacrificed at week 39. Animals on the NASH diet were randomized and either left on the NASH diet to serve as a vehicle control group, or treated daily for 8 Weeks, PO, with 10mg/kg Elafibranor (Genfit, Loos, France) or 30mg/kg Obeticholic Acid (Intercept Pharma, New York, NY USA). Five (5) age-matched, control mice were fed standard diet NIH-31M chow. Liver morphology, serum chemistry (liver panels) were examined and analyzed (Explora BioLabs, San Diego, CA, USA). Biopsied or whole mouse livers were fixed, processed, embedded, sectioned, mounted on slides and stained with Hematoxylin and Eosin (H&E), Masson’s trichrome (MTC), and Picrosirius red (PSR) using optimized and validated staining protocols (Reveal Biosciences, San Diego, CA, USA). Whole slide images were scanned and imaged under brightfield at 40x magnification with a 3DHISTECH PANNORAMIC™ FLASH 250 (EpreDia, Kalamazoo Michigan USA). The study design is summarized below.



Treatment	Timepoint	Number of Animals for 30, 39 Week Timepoints	Stains
Standard Diet (NIH-31M)	30, 39 Weeks	5, 5	H&E, MTC/PSR
NASH Diet	30, 39 Weeks	10, 5	H&E, MTC/PSR
NASH Diet + Elafibranor	39 Weeks	5	H&E, MTC/PSR
NASH Diet + Obeticholic Acid	39 Weeks	5	H&E, MTC/PSR

Highly quantitative data were generated using imageDx™ NASH (Reveal Biosciences), an automated, integrated workflow that analyzes and manages whole slide images. Figure 1 summarizes the process that Reveal Biosciences follows to obtain analysis data. Each whole slide image is first assessed for quality using a precise focal measurement followed by an accuracy check. All tissue and staining artifacts are digitally excluded from the reported quantification. The analysis process includes automated identification of tissue, followed by segmentation of regions of interest and then classification of stained positive and negative cells and structures for measurement of expression. The identified regions were then quantified for precise positivity.

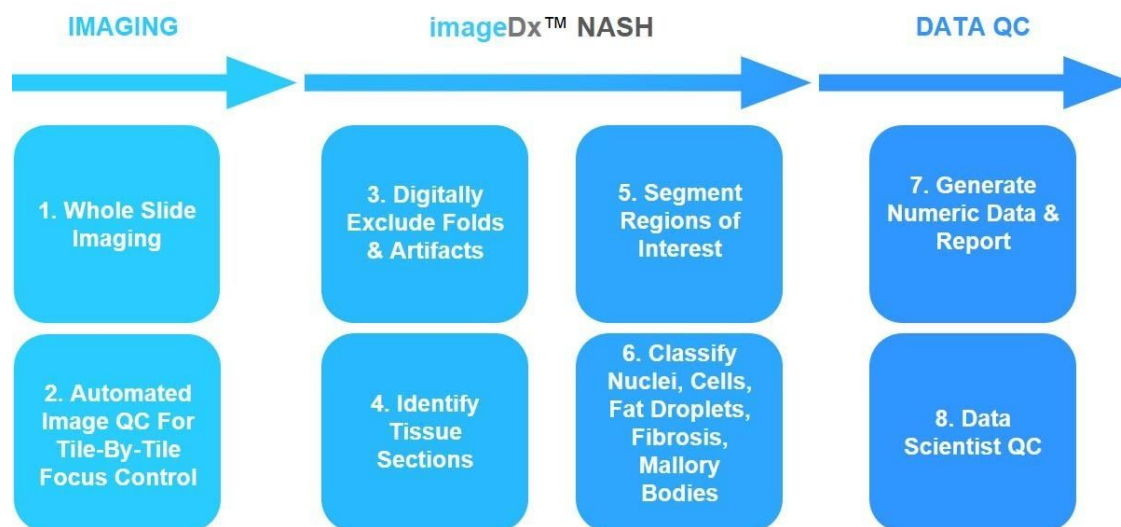


Figure 1. Reveal Bioscience Digital Assay Workflow

Images were quantified for steatosis (% by area, % macrovesicular and microvesicular, average vesicle size), inflammation (immune cell density, immune cell count), hepatocellular ballooning (ballooning hepatocyte density), presence or absence of Mallory bodies, fibrosis (% by area), as summarized below. A summary of numerical data from the quantitative imageDx™ NASH analysis is presented in the appendix.

Steatosis Analysis	The amount of total lipid accumulation, subcategorized into macro or micro vesicular, amount of lipid/hepatocyte, and the mean vesicle size within the entire section area analyzed of the H&E stained section.
Ballooning Hepatocyte Density	The density of ballooning hepatocytes within the entire section area analyzed of the H&E stained section.
Immune Cell Density	The total number of inflammatory cells and inflammatory cell density within the entire section area analyzed of the H&E stained section.
Fibrosis Percentage (%)	The amount of total fibrosis within the entire section area analyzed of the MTC or PSR stained section.
Mallory Bodies	The presence or absence of Mallory Bodies within the entire section area analyzed of the H&E section.
Tissue Area Analyzed (mm²)	The total tissue area used for analysis in the sample. This metric excludes any region classified as artifact, out of focus or otherwise purposely excluded from the analysis and is used for each feature analysis.

For microscopic evaluation of liver sections, a triple board-certified veterinary pathologist with experience in laboratory animals and toxicologic pathology evaluated the H&E, PSR, and MTC-stained slides. The H&E-stained sections were used to assess steatosis (fatty change), inflammation, hepatocellular ballooning, bile duct hyperplasia, and extramedullary hematopoiesis (EMH). The PSR and MTC-stained sections were evaluated for fibrosis, indicated by various shades of blue with darker blue indicating mature collagen and pale blue indicating newer or immature collagen. Samples submitted for evaluation included 2 sets of slides of liver biopsies (2 images each for livers stained with H&E and MTC or PSR stains).

RESULTS

Diet induced- NASH B6 mice exhibit increased body and liver weight

As shown in Figure 2, the diet-induced NASH mice fed the NASH diet exhibited significantly higher body weight compared to animals fed the standard control diet (2A). From a morphological standpoint, livers from the NASH diet animals appeared larger in size and lighter in color (2B), characteristic of NASH. Liver weights, normalized as a percentage of body weight, were well above those of control animals (2C).

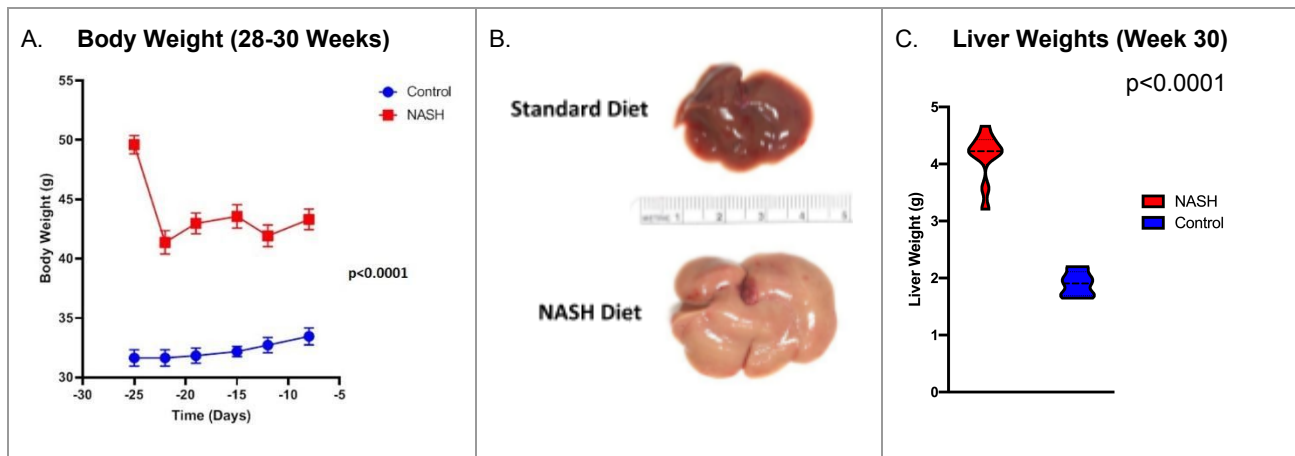


Figure 2. Characterization of NASH diet conditioned animals at 30-week timepoint shows (A) decrease in weight of NASH diet animals at arrival at study site followed by an increase in body weight through the 2-week acclimatization period. At the 30-week timepoint, NASH conditioned animals show significantly higher body weights compared to control diet animals ($p < 0.0001$, two-way ANOVA), (B) liver morphology with increased organ size of the NASH diet animals and (C) significant increase in liver weight compared to control diet animals ($p < 0.0001$, unpaired t-test).

Steatosis Analysis

For steatosis quantitation, lipid regions (white) within the H&E-stained slides were identified and quantitated as a percent of the total image analysis area. The algorithm first identified tissue areas on whole slide images followed by a more localized identification of positive lipid regions. Lipid regions are visualized by the blue mask overlaid onto the tissue (Figure 3A). The amount of lipid or steatosis was measured and expressed as a percentage of the total image analysis area. The amount of lipid was subcategorized into macrovesicular and microvesicular steatosis, as determined by lipid droplet size with a cutoff of $65 \mu\text{m}^2$ (Figure 3B). The percentage of steatosis area and macrovesicular steatosis in the NASH diet animal sections was significantly increased compared to that measured in the control diet animals at 30-weeks (Figure 3C). The full data set includes percent lipid area, total lipid area (mm^2), percent macrovesicular, percent microvesicular, average vesicle size (μm^2), lipid/hepatocyte, and tissue area analyzed (Appendix Tables 1-2). The precision of the steatosis quantification was measured by evaluating the mean lipid area and the mean vesicle size in triplicate with data at each experimental timepoint. Across control diet and NASH diet fed animals, the mean liver lipid area varied from 0.03-0.09% and 0.00-0.08% and the mean droplet size varied from 0.01-0.05% and 0.02-0.06%

respectively, indicating that the steatosis algorithms perform in a highly precise manner for the determination of lipid amount and mean droplet size with control and treated tissue section images.

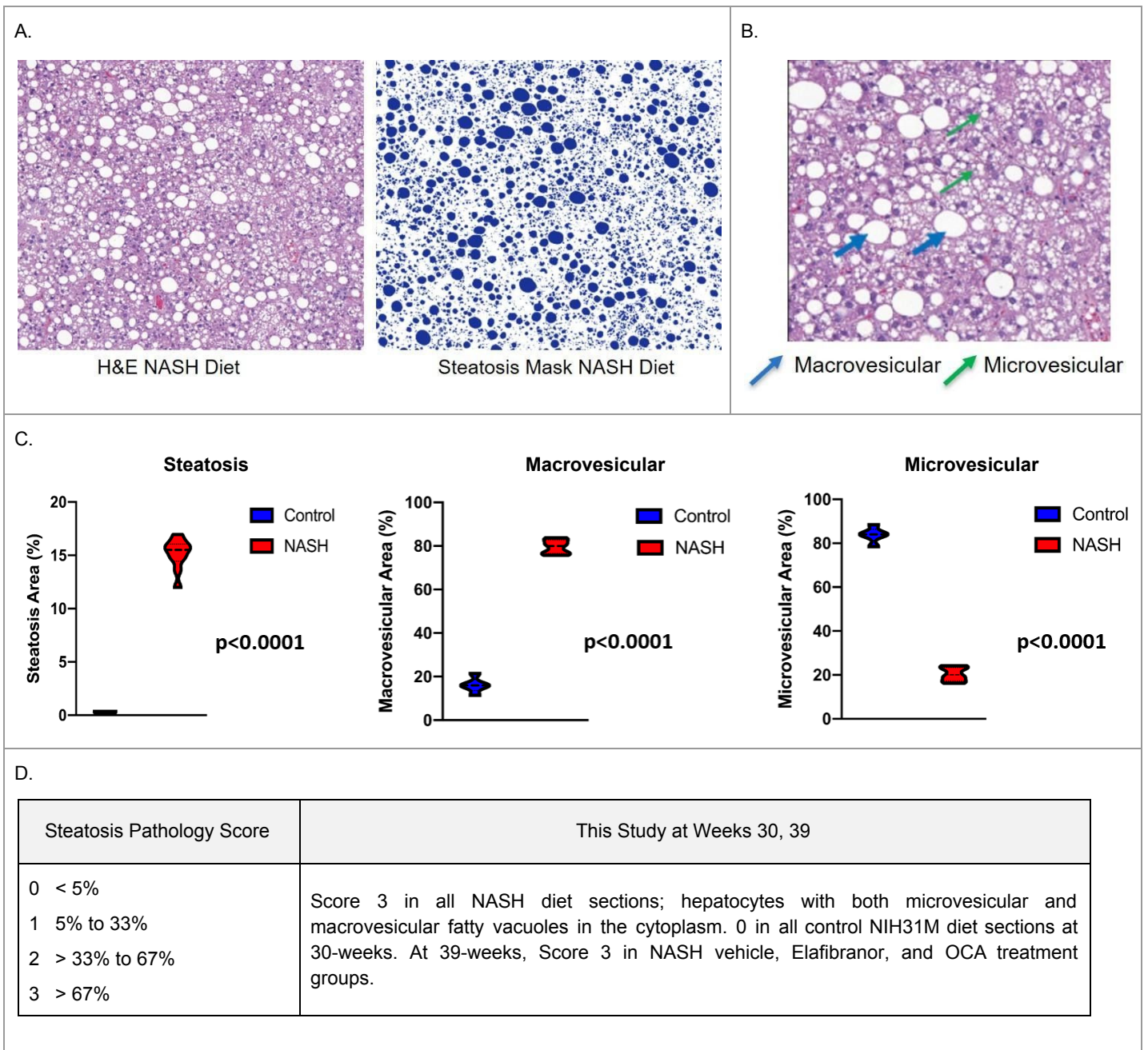


Figure 3. Steatosis analysis of NASH diet conditioned animals at 30-weeks (A) showing liver stained with H&E (A, left) and corresponding mask, the result of cell-by-cell segmentation (A, right) over the same section of tissue identifying cells positive for lipid accumulation (blue) used for quantification, (B) Hepatocytes with fatty change (steatosis); examples of macrovesicular (blue arrows) and microvesicular (green arrows) lipid accumulation within hepatocytes, all NASH diet sections showed similar pathology. (C) Quantitation of total percentage of steatosis shows markedly elevated amounts in NASH diet animals compared to control diet with significant differences in the amounts of macro- and micro-vesicular steatosis ($p < 0.0001$, unpaired t-test, all steatosis), (D) Pathologist description of steatosis and score summary for control, NASH, NASH with Elafibranor, and NASH with OCA treatment groups.

The results of the lipid quantitation show that the mean lipid per hepatocyte increased 80-fold from 3.31 μm^2 to 266.9 μm^2 in the animals fed the NASH versus the standard NIH-31M diet for 30 weeks (Figure 4A). The mean vesicle size increased more than 2-fold from 34.2 μm^2 to 76.0 μm^2 in the animals fed the NASH versus the standard NIH-31M diet (Appendix Tables 1,2). The animals fed the NASH diet mainly showed macrovesicular accumulation of lipid within hepatocytes versus the control diet group which primarily had very small microvesicular lipid inclusions within hepatocytes. At the 39-week timepoint (8 week treatment), the mean lipid per hepatocyte in the vehicle control NASH diet group was 212.16 μm^2 compared to 45.47 μm^2 and 78.53 μm^2 in the Elafibranor and the OCA treatment groups respectively indicating a significant reduction in the amount of lipid retained within hepatocytes with the liver samples (Figure 4B).

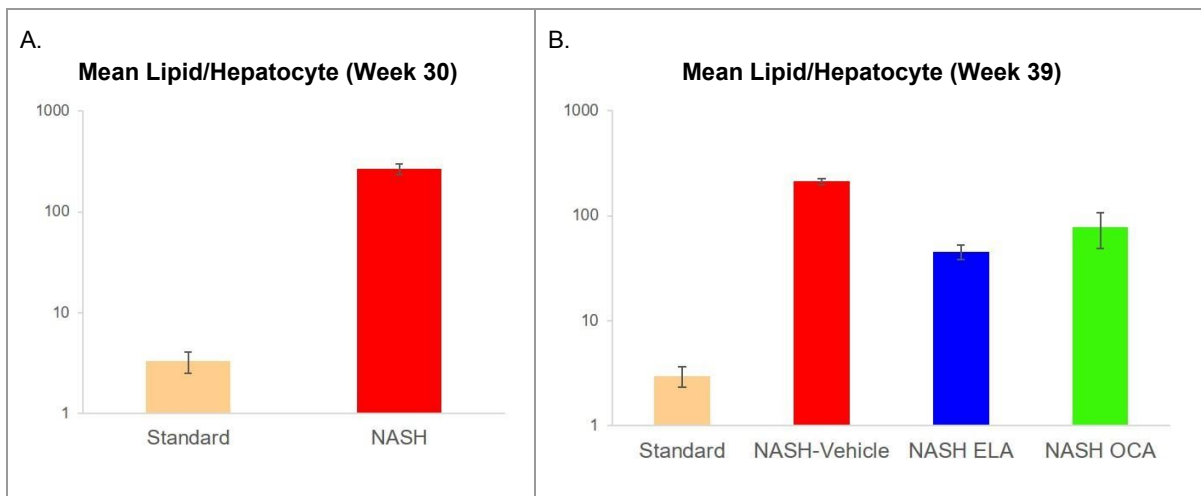


Figure 4. Mean lipid per hepatocyte (μm^2) averaged over entire whole slide image for all animals within control (n=5) or NASH diet groups (n=10) at 30-weeks (A) or post-treatment 39 weeks (B). (A) Mean lipid/hepatocyte increases significantly (80-fold) with NASH diet compared to standard NIH-31M diet ($p < 0.001$, unpaired t-test). (B) Mean lipid/hepatocyte in NASH Elafibranor and OCA-treated groups show significant decrease in the amount of lipid per hepatocyte compared to the NASH diet vehicle control group at 39-weeks ($p < 0.0001$, unpaired t-test).

The pathologist NAS score for steatosis is based on the number of hepatocytes with either macrovesicular and/or microvesicular hepatocellular fatty vacuoles. Steatosis (hepatocellular fatty change) was a notable feature of the livers in this study. Fatty vacuoles were seen as clear intracytoplasmic vacuoles with clear, intact edges. Microvesicular fatty vacuoles were seen as approximately 1 μm or smaller single or multiple vacuoles; macrovesicular vacuoles were seen as 3 μm or larger and often single but sometimes multiple within the same cell. Many of the fatty vacuoles seen were microvesicular. At the 30-week timepoint, the NIH-31M control diet fed animals scored a 0 and the NASH diet fed animals scored a 3, indicating either less than 5% steatosis or more than 67% steatosis respectively (Figure 3D). Within each of these groups, the pathologist-derived score was consistent for all animals. At this timepoint, the average of the AI-derived lipid area expressed as a percentage of tissue area analyzed for control diet animals was 0.31% and 15.1% for NASH diet animals showing a similar trend to the pathologist-reported lipid percentages but a gross correlation with actual percentage values per group (ex. the NASH diet group with AI-reported value of 15.1% vs. pathologist-reported value of greater than 67%). At the 39-week timepoint, pathologist-reported steatosis was more than 67% for the NASH vehicle and NASH diet groups treated with Elafibranor and OCA (Score 3) while the AI-derived lipid percentages were 13.2% for NASH vehicle, 3.1% for NASH with Elafibranor and 6.6% for NASH with OCA treatment. The AI-measured difference in lipid percentages for the vehicle and the Elafibranor and OCA-treated groups was significant ($p < 0.01$, unpaired t-test) and in comparison to the pathologist-reported scores, shows that the AI-driven approach provides a more sensitive measurement of lipid change in untreated and treated tissue sections.

Hepatocyte Ballooning Analysis

Ballooning hepatocytes were identified and quantitated as the number of ballooning cells within the total image analysis area of H&E-stained liver sections. The algorithm first identified tissue areas on whole slide images followed by positive ballooned cells based on the cell diameter and presence of disrupted cytoskeletal structure, an example is shown (blue box, Figure 5A). The full data set includes the density of ballooning hepatocytes (cells/cm²), and the tissue area analyzed (mm²) (Appendix Tables 3&4).

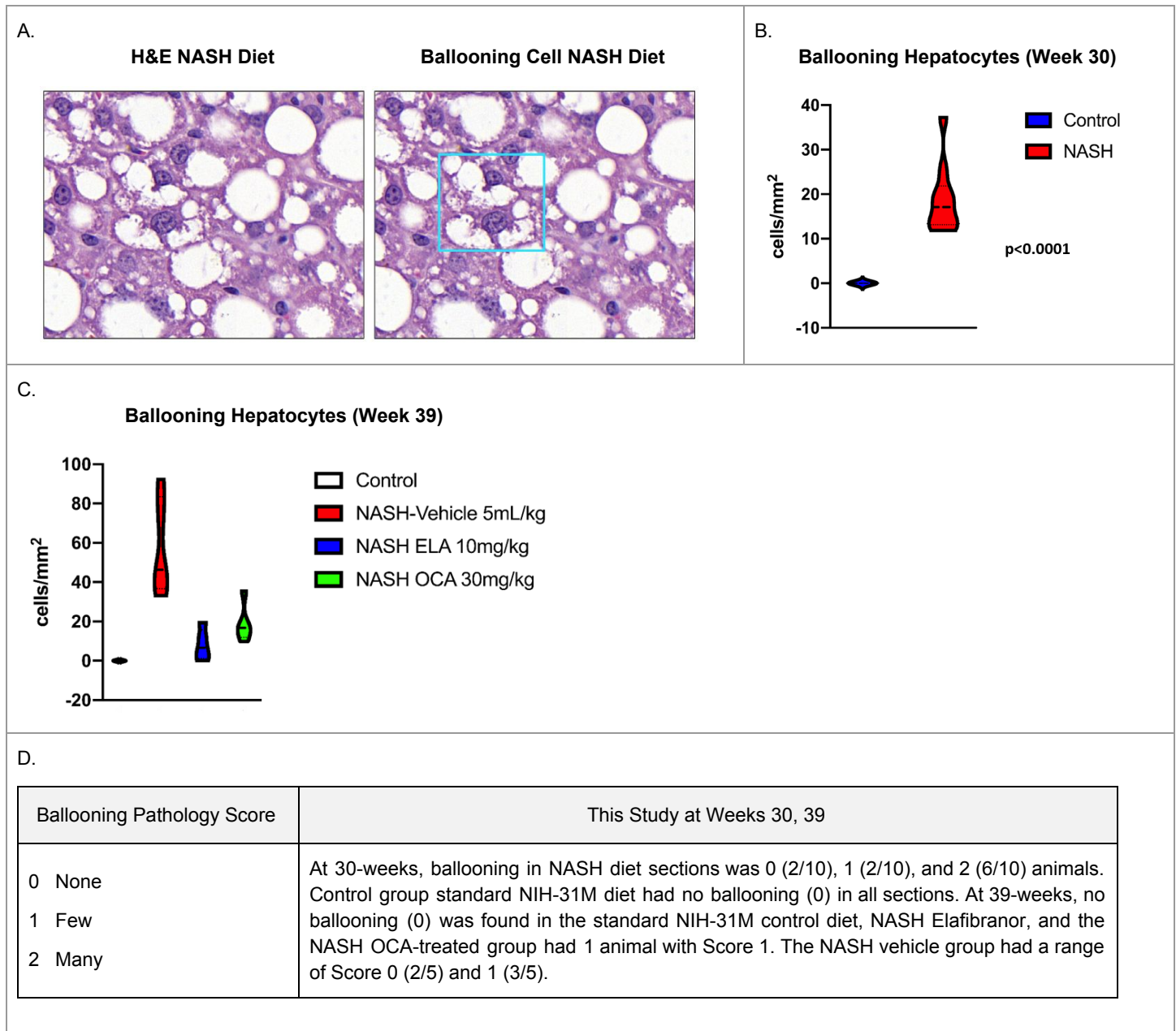


Figure 5. Hepatocyte ballooning analysis of NASH diet conditioned animals at 30-weeks (A) showing liver stained with H&E (A, left) and corresponding blue box, the result of cell-by-cell segmentation (A, right) over the same section of tissue identifying cells positive for ballooning across the entire whole slide image used for quantification. (B) Quantitation of the frequency of ballooning hepatocytes shows markedly elevated numbers in NASH diet animals compared to control diet ($p < 0.0001$, unpaired t-test) at 30-weeks (C) At week-39, frequency of ballooning hepatocytes is increased in NASH diet vehicle group compared to control diet ($p < 0.001$, unpaired t-test), frequency of ballooning hepatocytes is decreased in the NASH Elafibranor and OCA-treated groups compared to NASH diet vehicle group following treatment ($p < 0.001$ and $p < 0.05$ respectively, unpaired t-test) (D) Pathologist description of ballooning and score summary for control, NASH diet, NASH Elafibranor, and OCA-treated groups.

The results of the ballooning hepatocyte analysis show that in both the 30- and the 39-week studies, there are negligible numbers of ballooning hepatocytes within the standard diet (NIH-31M) control groups at both timepoints (Figure 5B and 5C). Within the NASH diet groups, the 30-week group had a mean ballooning hepatocyte density of 18.82 cells/cm² while the NASH diet vehicle control group at the 39-week timepoint had a mean ballooning hepatocyte density of 57.32 cells/cm² which shows an increase in numbers of ballooning hepatocytes during the 8-week treatment period during which animals are fed the NASH diet and hepatocytes are accumulating lipid which is causing cytoskeletal injury and the resultant ballooning phenotype. The 8-week treatment of NASH diet animals with both Elafibranor and OCA significantly reduced the frequency of ballooning cells to 8.15 cells/cm² and 18.86 cells/cm² compared to the NASH vehicle diet group (57.32 cells/cm²).

The pathologist description of hepatocyte pathology was reported as a range of changes, from marked hydropic degeneration with lacy indistinct intracytoplasmic vacuoles, to greatly expanded cells with degenerate or no nuclei, to loss of cells with only faint (ghost) outlines of cells remaining (Figure 5D). Cells with loss of nuclei or very pale or condensed nuclei and/or obvious cytoplasmic enlargement with notable cell debris were indicative of necrosis. Within the 30-week timepoint, the pathologist-assigned ballooning score was 0 for all animals on the standard NIH-31M diet and varied from 0 (2 animals), 1 (2 animals) to 2 (6 animals) for those on the NASH diet (Figure 5B). In comparison, AI-derived ballooning hepatocyte densities were 0 for animals on the NIH-31M diet and averaged 18.82 cells/cm² for those animals fed the NASH diet. Within the NASH diet group, the ballooning hepatocyte density ranged from 11.84 to 37.29 cells/cm² showing the amount of individual animal variation that can be measured using the AI-derived method versus a numerical score with poor definition of the difference between scores. Within the Elafibranor and OCA treatment groups at the 39-week timepoint, the pathologist ballooning hepatocyte scores were mostly 0 with a single animal scored 1. The AI-derived quantitation of hepatocyte ballooning density showed an average of 57.32 cells/cm² in the NASH diet vehicle group, 8.15 cells/cm² in the Elafibranor group and 18.86 cells/cm² in the OCA treatment group, which provides a more granular and quantitative measurement of the amount of hepatocyte damage than is reflected in the 0-2 CRN ballooning scoring system (Figure 5D).

Mallory Bodies Analysis

Mallory bodies were identified and quantitated within H&E-stained liver sections as the presence of Mallory bodies within the total image analysis area. The algorithm first identified tissue areas on whole slide images followed by positive Mallory bodies visualized by the overlaid purple mask (Figure 6). The presence or absence of Mallory bodies is reported in tables 3&4 in the Appendix. For most of the NASH diet groups at both the 30- and 38-week timepoints, most cases have one or more hepatocytes with Mallory-Denk bodies. The control diet group (NIH-31M) did not have ballooning hepatocytes.

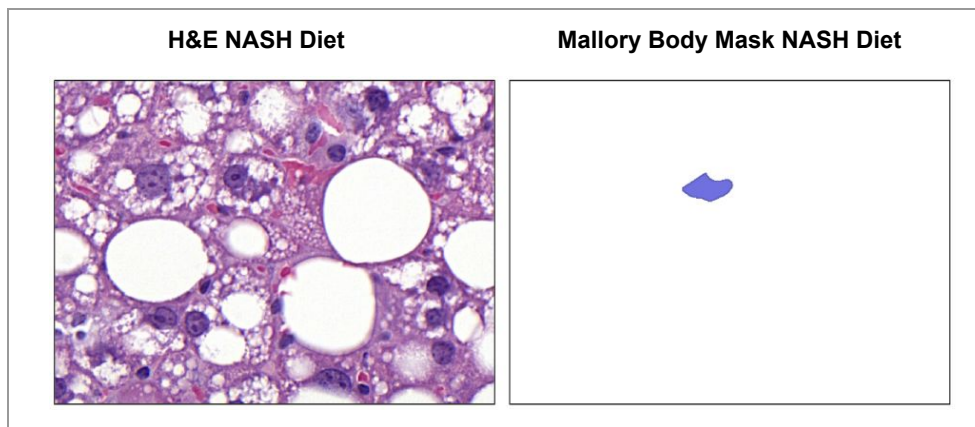


Figure 6. Mallory body analysis of NASH diet-conditioned animals at 30-weeks (A) showing liver stained with H&E (left) and corresponding purple mask, the result of cell-by-cell segmentation (right) over the same section of tissue identifying positive ballooning cells across the entire whole slide image used for quantification.

Inflammatory Cell Analysis

Inflammatory cells were identified and quantitated within H&E-stained liver sections as the number of immune cells within the total image analysis area. The algorithm first identified tissue areas on whole slide images followed by positive immune cells visualized by the overlaid red mask (Figure 7A). The full data set includes immune cell density (cells/mm²), total area of immune cells (mm²), and total number of inflammatory cells within the entire tissue area analyzed. The number of immune cells was counted and measured as the total amount of immune cells. (Appendix Table 5&6).

The results of the inflammatory cell analysis at the 30-week timepoint showed a modest 1.2-fold increase in the immune cell density between the control diet group (NIH-31M) and the NASH diet group (Figure 7C). At the 39-week timepoint, this trend continued with the vehicle control NASH diet group having a 1.5-fold increase in the immune cell density over that of the control diet group (Figure 7D). Following the 8-week treatment, the density of immune cells in the Elafibranor treatment group did not show a significant change from that of the vehicle control NASH diet group (508.8 cells/mm² vs. 617.8 cells/mm²). 8-week OCA treatment group showed a significantly reduced immune cell density (490.8 cells/mm²) compared to the levels of immune cells measured in the vehicle control NASH diet group (617.8 cells/mm²)(Figure 7D).

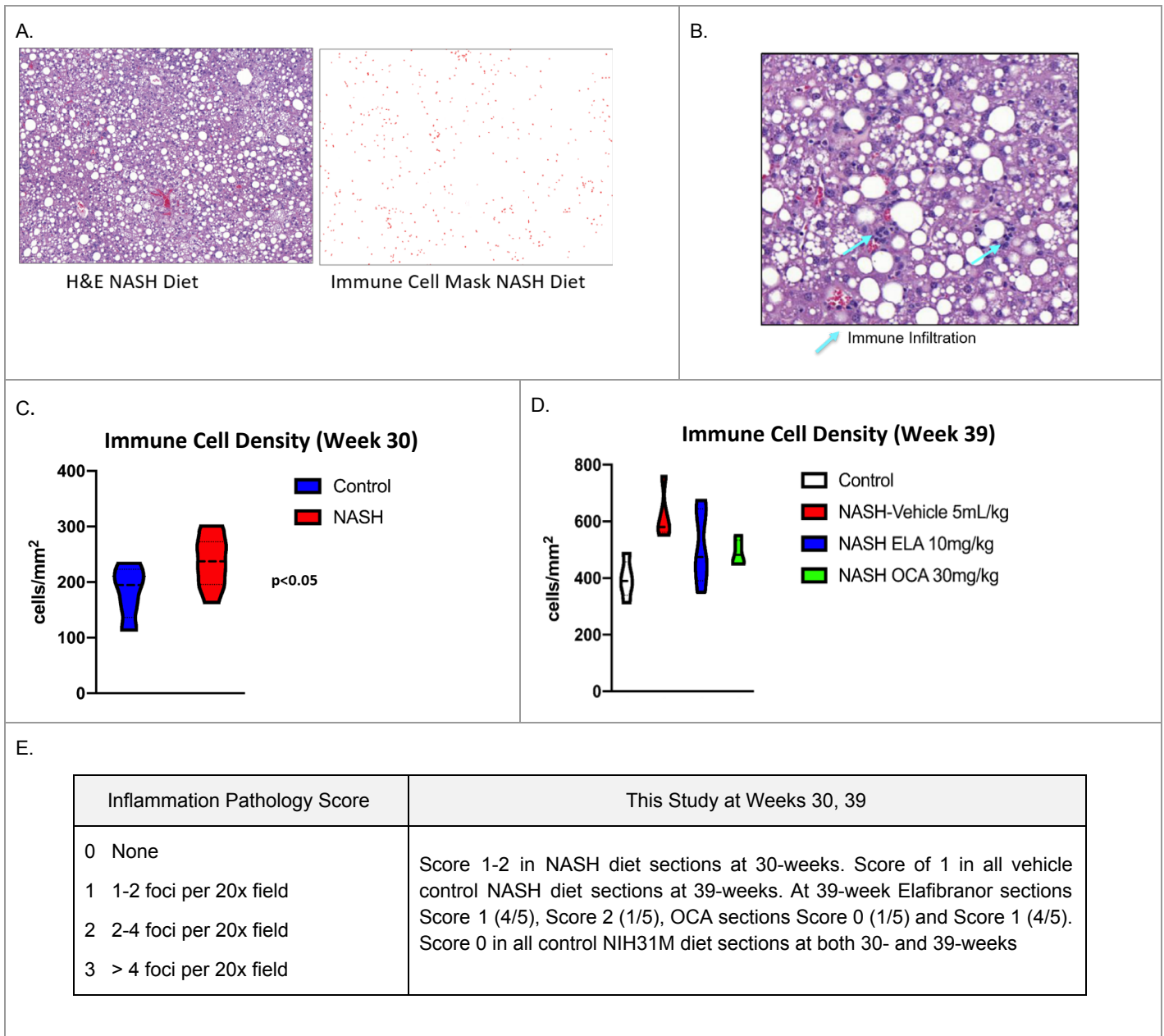


Figure 7. Inflammatory cell analysis of NASH diet conditioned animals at 30-weeks (A) showing liver stained with H&E (A, left) and corresponding mask, the result of cell-by-cell segmentation (A, right) over the same section of tissue identifying immune cells (red) used for quantification, (B) immune infiltration of lobular regions; examples of immune cell foci (blue arrows) adjacent to steatotic hepatocytes, all NASH diet sections showed similar immune infiltration, (C) Quantitation of immune cell numbers show increased numbers of immune cells in NASH diet animals compared to control diet ($p < 0.05$, unpaired t-test), (D) Quantitation of immune cell numbers at 39-weeks shows increased numbers of immune cells maintained in the NASH diet vehicle control group and that 8-week treatment with OCA results in a significant decrease in the number of immune cells ($p < 0.05$, unpaired t-test). Treatment with Elafibranor does not result in a significant decrease of immune cells ($p > 0.05$, unpaired t-test) compared to the vehicle NASH diet group, (E) Pathologist description of inflammation and score summary for control, NASH, NASH with Elafibranor, and NASH with OCA treatment groups.

The pathologist score for inflammation included infiltrates of leukocytes such as macrophages, lymphocytes, and neutrophils, seen primarily along the hepatic sinusoids and foci consisted of two to three leukocytes. Findings within the NASH diet group were primarily small patchy foci within the liver lobules and no significant foci were noted in the control diet group (CRN scores 1-2 and 0 respectively, Figure 7E)). Quantitative measure of the immune cell density (averages) within the NASH diet group at 30-weeks was 237.0 cells/mm² and within the control diet group was 182.8 cells/mm² which mirrors the pathologist-assigned CRN scores of 1-2 for the NASH diet group and 0 for control diet group (Figure 7C, E). At the 39-week timepoint the averaged CRN inflammation score was 0 for the NIH-31M diet, 1 for the vehicle control NASH diet group, 1.2 for the Elafibranor group, and 0.8 for the OCA group. The quantitated immune cell density measurements correlate well with the average CRN inflammation scores for the control diet, vehicle NASH, NASH Elafibranor, and the NASH OCA treatment groups (Figure 7D, E). Examination of individual animals with quantitative immune cell density measurements gives a more in-depth, detailed assessment of incremental phenotypic changes and responses to diet-induced inflammation and treatments.

Fibrosis Analysis

For fibrosis analysis, collagen and extracellular matrix fibers within Picosirius red-stained liver sections were identified and quantitated as a percent of the total image analysis area. The algorithm first identified tissue areas on whole slide images followed by positive collagen fiber regions (appear red) visualized by the overlaid green mask (Figure 8A). The amount and intensity of collagen or fibrosis staining was measured and expressed in relation to the total image analysis area. The full data set includes total fibrosis (%), and total amount of fibrosis within the entire tissue area analyzed (mm²) (Appendix Tables 7&8).

The results of the quantitative fibrosis measurement for the 30-week timepoint showed significantly more fibrosis area in the NASH diet animals 9.30%, in comparison to 2.59% in the control (NIH-31M) diet group ($p < 0.001$, unpaired t-test). At the 39-week timepoint, animals fed the vehicle NASH diet had a 4.5-fold increase in the mean amount of fibrosis area compared to animals fed the control (NIH-31M) diet. Within the treatment groups, the Elafibranor-treated group showed a significant decrease in the mean fibrosis area (2.90%) compared to the NASH diet vehicle group (5.31%) ($p < 0.05$, unpaired t-test). In the OCA-treated group, the mean fibrosis area was 1.5-fold lower than the mean fibrosis area of the NASH diet group although this was not statistically significant.

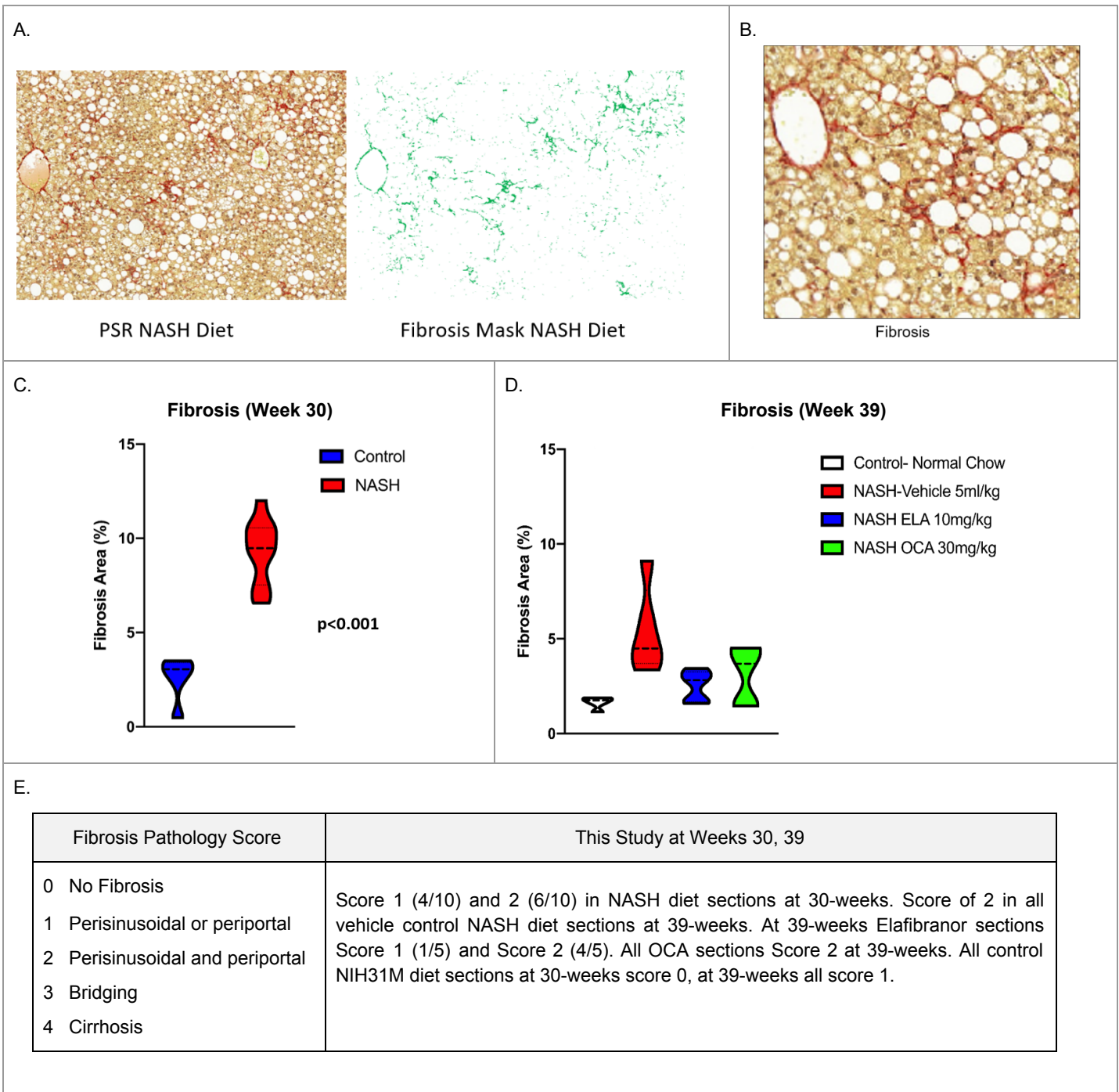


Figure 8. Fibrosis analysis of NASH diet conditioned animals at 30-weeks (A) showing liver stained with Picrosirius red (A, left) and corresponding mask (A, right) over the same section of tissue identifying regions of fibrosis used for quantification, (B) Magnified view of fibrotic region (stained red) showing positive perisinusoidal and periportal staining of collagen fibers, (C) Quantification of fibrosis percentage at 30-weeks shows an increased amount of fibrosis in the NASH diet animals compared to the control diet group ($p < 0.001$, unpaired t-test), (D) Quantification of the amount of fibrosis at 39-weeks shows increased fibrosis in the vehicle NASH diet control group compared to the control diet group ($p < 0.001$, unpaired t-test). Treatment with Elafibranor significantly reduces the amount of fibrosis compared to the NASH diet vehicle control group ($p < 0.05$, unpaired t-test). Treatment with OCA does not significantly decrease the amount of fibrosis compared to the vehicle NASH diet group, (E) Pathologist description of fibrosis and score summary for control, NASH, NASH with Elafibranor, and NASH with OCA treatment groups.

The pathologist score for fibrosis indicates the presence of fibrosis, mainly composed of collagen, but not the quality or thickness of the fibrous connective tissue. Within the 30-week NASH diet group 40% of the animals had periportal or perisinusoidal fibrosis (Score 1) with 60% of the animals having periportal and perisinusoidal fibrosis (Score 2). As expected, the AI-derived quantitative total fibrosis percentages in the NASH diet and the control diet animals correlated with the reported pathologist-derived fibrosis scores. The animals on the control (NIH31M) diet had no fibrosis (Score 0) at the 30-week timepoint, and at the 39-week timepoint were reported to have mild perisinusoidal or periportal fibrosis (Score 1). The quantitative analysis of the average fibrosis percentage of the control NIH31M diet group shows a lower amount of fibrosis 1.18% at the 39-week timepoint compared to the 30-week timepoint (2.59%). It is likely that the measured fibrosis percentage does not correlate well with the pathologist-reported fibrosis scores since these scores primarily represent a distribution or pattern of staining within the sample compared to a measurement of the amount of fibrosis. Measured differences in the amount of average fibrosis percentages within the control diet groups at the 30- and 39-week timepoints could be due to differences in the stain intensity, sampling variability due to the liver region, limited sample size, or may represent actual differences in the baseline levels of collagen. At the 39-week timepoint, all of the NASH diet vehicle animals had perisinusoidal and periportal fibrosis (Score 2). The Elafibranor-treated group had some decrease in fibrosis (20% with Score 1 and 80% with Score 2), and the OCA-treated group (all Score 2) did not show a difference from that of the NASH diet vehicle control group (all Score 2). In contrast to the reported similar CRN fibrosis scores for NASH diet and Elafibranor treatment, the quantitative fibrosis measurement showed a significant more than 2-fold decrease in the amount of fibrosis following Elafibranor treatment ($p < 0.05$, unpaired t-test).

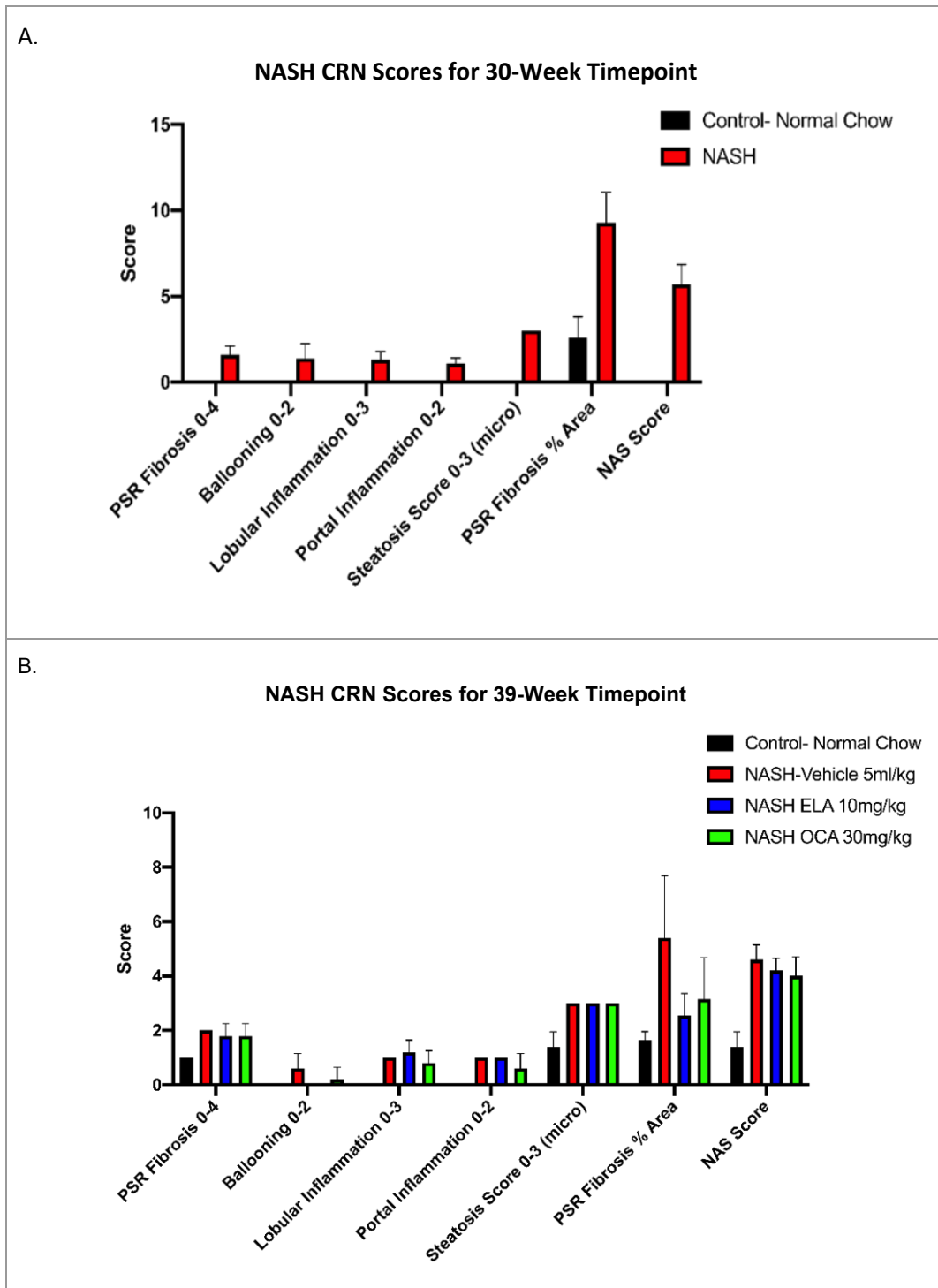


Figure 9. Summary of NASH CRN scores for the 30-week (A) and the 39-week (B) timepoints, (A) Scores for NASH diet group are significantly increased across all histologic features except portal inflammation in comparison to the control diet group (PSR fibrosis $p < 0.01$, ballooning $p < 0.01$, lobular inflammation $p < 0.05$, steatosis $p < 0.0001$, fibrosis $p < 0.0001$, NAS score $p < 0.0001$, two-way ANOVA), (B) Scores for NASH diet vehicle group are significantly higher in comparison to the control diet group for steatosis ($p < 0.001$), fibrosis ($p < 0.0001$) and the NAS score ($p < 0.0001$)(all two-way ANOVA). The Elafibranor and the OCA treatment groups had significantly lower fibrosis than the NASH diet vehicle control group ($p < 0.0001$, two-way ANOVA).

Effects of NASH Treatments on Body Weights and Biomarker Analysis

The effects of the dual PPAR- α/δ agonist Elafibranor and FXR agonist Obeticholic Acid, two different stage III clinical NASH drug treatments, were analyzed in the standard and NASH diet mice. As illustrated in Figure 10, the body weights of the Elafibranor, OCA and NASH vehicle mice all started about 5 grams higher than that of the standard diet control mice. Once treatment began, the NASH mouse weights responded uniquely to the treatments. Whereas the Elafibranor-treated NASH mice lost weight and eventually weighed less than the standard diet mice at study termination, the OCA-treated mice gained weight at a rate higher than that of the NASH diet vehicle mice (Figure 10A). Conversely, liver weights for the Elafibranor-treated NASH mice ended up higher than those of the OCA-treated and NASH diet vehicle mice, with similar trends when liver weights were normalized to percent of body weight (Figure 10B).

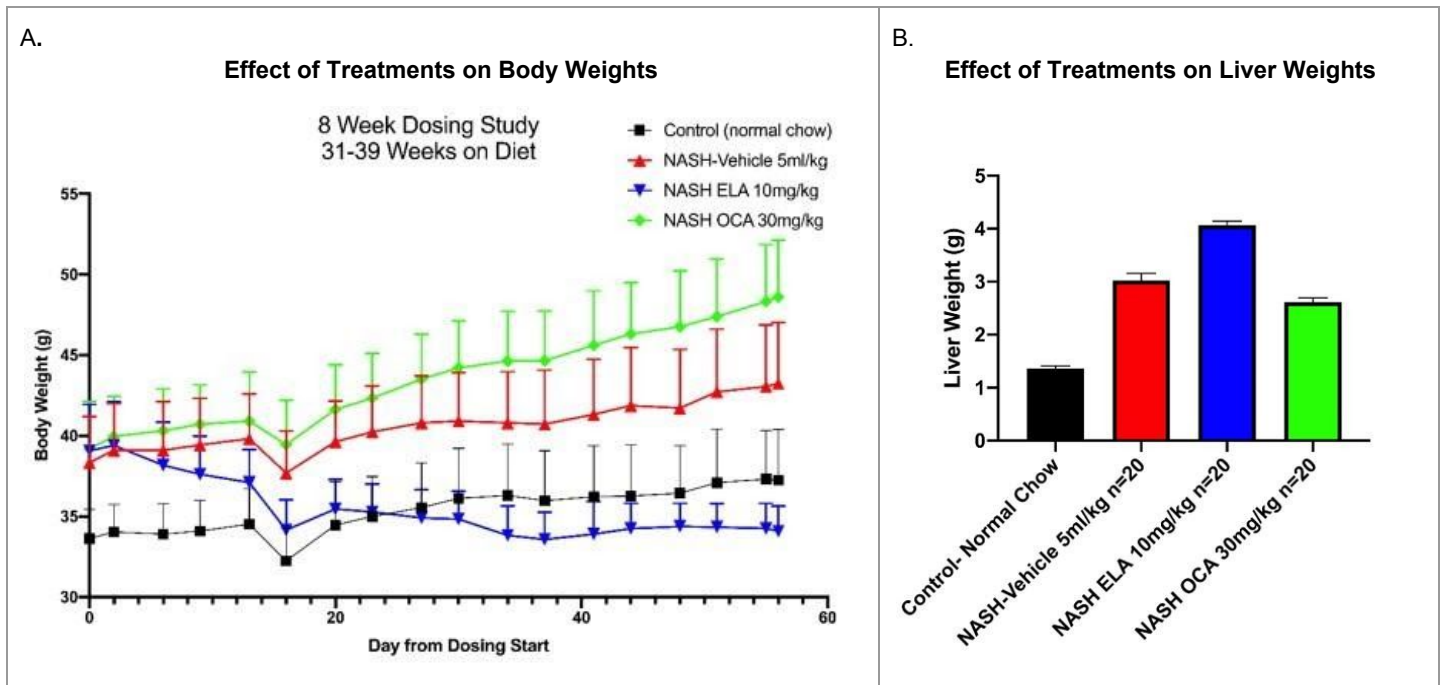


Figure 10. Effect of Treatments on Body and Liver Weights of standard NIH-31M and NASH Diet Mice (A) Comparison of body weight over the course of 8-week treatment of Elafibranor- and OCA-NASH mice. At 39-weeks the NASH diet vehicle group, the Elafibranor- and the OCA-treated groups showed significant increase in body weight compared to the standard diet group ($p < 0.001$, two-way ANOVA), (B) Comparison of liver weight at 39-weeks, the NASH diet vehicle group ($p < 0.0001$), the Elafibranor- ($p < 0.0001$) and the OCA-treated ($p < 0.05$) groups showed significant increase in liver weight compared to the standard diet mice (two-way ANOVA).

Following treatment with Elafibranor and OCA, the levels of circulating hepatic biomarkers including ALT, bilirubin, albumin and total cholesterol were measured (Figure 11). The levels of ALT were significantly reduced in response to Elafibranor and OCA treatment ($p < 0.0001$ and $p < 0.05$ respectively). Total cholesterol levels were decreased in the Elafibranor- and OCA-treated animals in comparison to the standard diet and NASH diet mice ($p < 0.001$ and $p < 0.0001$ respectively). The Elafibranor and OCA treatments had no effect on the total bilirubin levels but did show some significant increase in the amount of albumin ($p < 0.0001$ and $p < 0.05$ respectively).

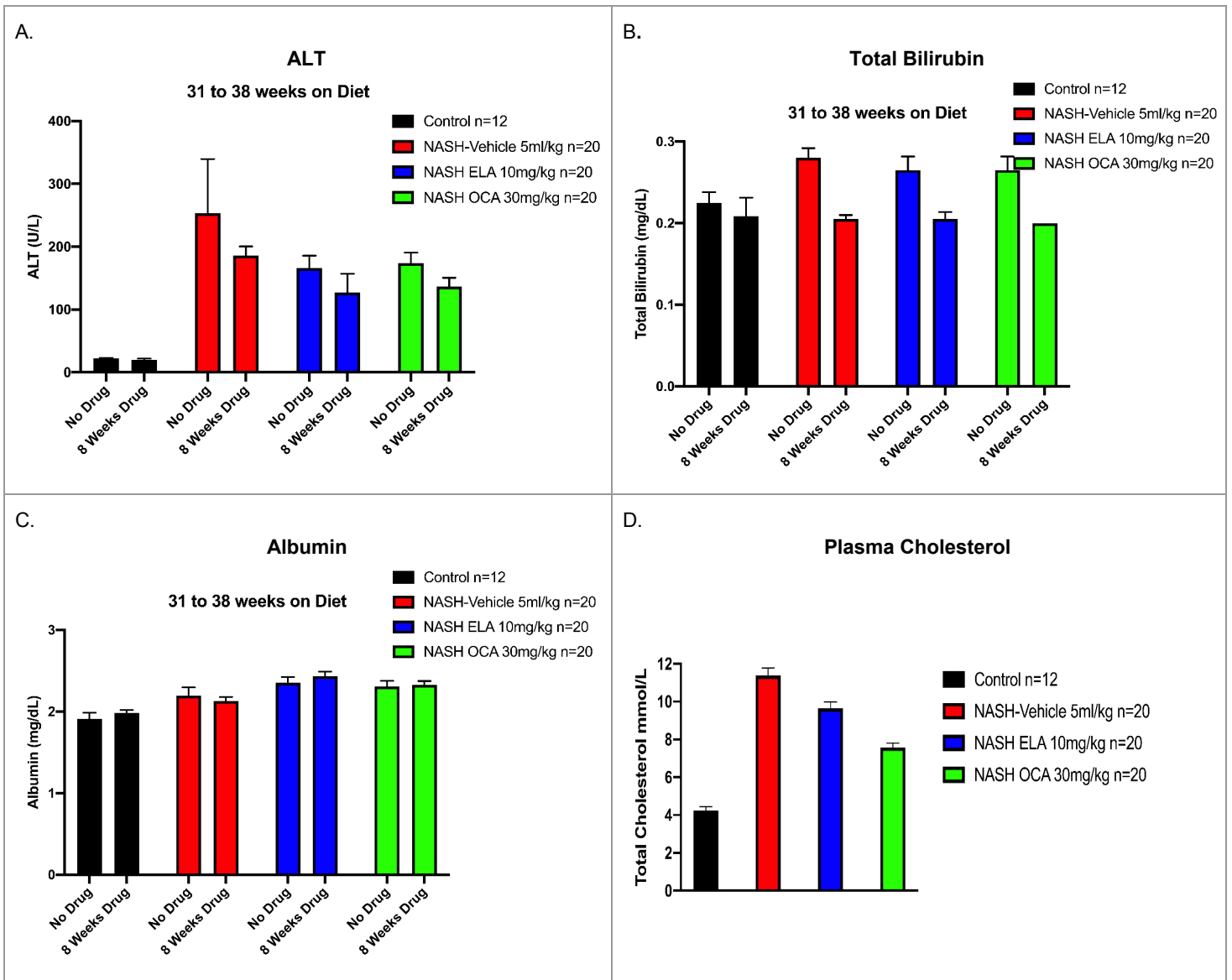


Figure 11. Effect of NASH Therapeutics on Biomarkers for Liver Disorder and Hyperlipidemia in NASH Diet and control Mice (A) ALT levels of NASH diet vehicle to standard control group showed significantly increased levels at both 31-weeks and 39-weeks ($p < 0.001$ and $p < 0.05$, two-way ANOVA), (B) Bilirubin levels of NASH diet vehicle compared to standard control group showed significantly higher levels at 31-weeks ($p < 0.05$, two-way ANOVA), (C) Albumin levels showed a significant increase at 39-weeks with both Elafibranor and OCA-treatment compared to NASH diet vehicle group animals ($p < 0.0001$ and $p < 0.05$, two-way ANOVA) (D) Plasma cholesterol levels at 39-weeks show increased cholesterol levels in NASH diet vehicle compared to standard control group ($p < 0.001$, two-way ANOVA), Elafibranor-treated ($p < 0.001$), and OCA-treated ($p < 0.0001$) compared to the NASH diet vehicle group (two-way ANOVA).

DISCUSSION

This study served two purposes, to characterize the relevant pathological features of the novel off-the-shelf, diet-induced mouse NASH B6 Model (Taconic Biosciences, Inc.) at baseline and during use in pre-clinical drug experiments (Explora BioLabs), and to demonstrate the sensitivity and utility associated with the imageDx NASH digital assay (Reveal Biosciences). Two timepoints were selected for analysis, including the 30-week mark to establish a baseline for measurement of the diet-induced phenotype, and then following an 8-week treatment regimen (39-week timepoint) with drug candidates at which time steatosis, inflammation, hepatocyte ballooning, and fibrosis were assessed. Qualitative (human) pathology examination described normal morphology and features in the liver sections from the animals fed the standard control diet, but those animals fed the NASH diet exhibited various disease related abnormalities. Under the conditions of this study, all NASH diet liver sections similarly showed prominent steatosis with minimal to mild inflammation, minimal ballooning and bile duct changes, and prominent fibrosis in MTC-stained sections, all of which was supported by the results of the digital quantitation assay.

Two drug candidates in phase III clinical trials were utilized to confirm the response of diet conditioned NASH mice to therapeutic treatment. Elafibranor, a known dual PPAR- α/δ agonist, and documented positive effector of insulin sensitivity and liver injury through anti-inflammatory and anti-fibrotic mechanisms, was given to mice on the NASH diet at 30-weeks and outcome measured at 39-weeks. The second candidate, obeticholic acid, a farnesoid X receptor (FXR) agonist, has been documented to improve insulin sensitivity and to exhibit both anti-inflammatory and anti-fibrotic properties, as well as to improve liver biomarkers. In this study, the C57BL/6NTac mice fed a high fat modified AMLN (NASH) diet displayed increased liver and body weights, and high serum levels of liver disease biomarkers. These animals exhibited features of NASH, including fatty liver, steatosis, inflammation, hepatocyte ballooning, and fibrosis. Treatment of the NASH diet-conditioned C57BL/6NTac mice with the stage III clinical NASH drugs improved overall liver profiles. Both OCA and Elafibranor reduced hyperlipidemia/total cholesterol and serum ALT levels. OCA treatment also lowered liver weight in proportion to body weight. Elafibranor possibly increased insulin sensitivity, and from morphological observation, reduced body weight and fat content. Importantly, the off-the-shelf NASH B6

mice provide a cost-effective and time-saving solution for preclinical NASH researchers, with their recapitulation of the multi-factorial NASH phenotype and relatable treatment responses to Elafibranor and OCA.

Throughout the study, we sought to present the quantitative results of the digital NASH assay in an objective manner in comparison to the more subjective, qualitative assessments of an albeit very experienced veterinary pathologist. The subjective nature of the pathologist's assessment of pathology is most evident in the recording of steatosis scores. Within control diet and NASH diet conditioned groups, both the assigned CRN steatosis scores and the algorithm-based quantitative results are consistent and correlate to the CRN steatosis score, but the represented lipid percentages differ. For example, an assigned CRN steatosis score of 3 for the NASH diet group represents an estimated lipid percentage greater than 67% and yet the corresponding AI-derived percent lipid area for these same tissues is measured and reported at 15.1%. This difference in lipid amount is reproducible across all studies and species to date and is likely due to both the difficulty in estimating lipid percentages by eye and the lack of a continuous scoring system that would allow for a more granular measurement similar to those generated with the AI-derived algorithms.

The quantitative output of the imageDx NASH digital assay provides a highly reproducible and scaled measurement of pathological features. To assign the CRN ballooning hepatocyte score, the pathologist is required to estimate the number of ballooning cells. This task can be hindered by the process of estimating instead of counting the number of cells that exhibit the hallmark visual characteristics of a ballooning cell (cytoskeletal damage and size features), and vagueness of visual characteristics in the score label (0 none, 1 few, 2 many). One can surmise that these labels could mean different numbers of ballooning cells within the same samples depending on the individual reading the slide. Ballooning cell measurements of none, few, or many are not granular enough to provide useful information in assessing the extent of the pathology occurring in the samples. Some have questioned the inclusion of ballooning hepatocyte analysis in rodent NASH models. Interestingly, the use of the quantitative NASH digital assay can assist with assigning a very consistent measurement of number of cells with positive criteria (cytoskeletal changes and large size) and could provide a better method for not only identifying the number of

ballooning cells, but also the location of these damaged cells within the tissue and in relation to immune cell populations.

Together, the results published within this study contribute to the successful validation of the world's first commercial, off-the-shelf mouse NASH model and the quantitative measurement of phenotype using imageDx NASH digital assay. The development of highly reproducible and sensitive computational models provide an effective approach to identifying small differences in tissue morphology that may not be easily discernible by visual examination. Combined efforts included the

advanced mouse development model, *in vivo* study management with surgeries and tissue collection, *in vitro* analysis, pathology, histopathology, digital whole slide scanning, and AI-based digital image analysis to quantify fibrosis, steatosis, inflammation, hepatocellular ballooning, and the presence of Mallory bodies. This off-the-shelf NASH B6 rodent model successfully recapitulates pathologic changes in NASH patients, and combined with imageDx NASH digital assay, provides pre-clinical researchers with an easy, reproducible, accurate and cost effective end-to-end solution for the development of effective NASH therapeutics.

ACKNOWLEDGMENT

The authors acknowledge the contributions of our collaborators at Taconic Biosciences, Explora BioLabs, Epredia, as well as the expertise of Dr. Mary E.P. Goad for pathology review and scoring of animals, K. Murugesan for data analysis, and M. Sanchez for data preparation.

APPENDIX

QUANTIFICATION

Table 1. Steatosis Analysis Summary 30-Weeks (Baseline)

Data for the 30-week timepoint with the control (standard NIH-31M diet) and the NASH diet conditioned group (NASH diet) showing total lipid area as well as more granular lipid data such as amount and type for individual hepatocytes.

Treatment	Sample	% Lipid Area	Mean Lipid per Hepatocyte (um ²)	Total Lipid Area (mm ²)	Total Number of Hepatocytes	% Macrovesicular	% Microvesicular	Mean Vesicle Size (um ²)	Tissue Area Analyzed (mm ²)
NIH-31M Diet	19-771 201 STND	0.26	2.86	0.27	95148	21.53	78.47	34.90	103.24
	19-771 202 STND	0.37	3.12	0.27	87131	15.72	84.28	28.20	74.16
	19-771 204 STND	0.36	4.36	0.31	70749	11.46	88.54	48.57	84.86
	19-771 214 STND	0.22	2.37	0.27	112757	16.06	83.94	33.03	120.29
	19-771 215 STND	0.31	3.84	0.28	72710	15.98	84.02	26.32	89.64
NASH Diet	19-771 121 NASH	14.86	240.00	7.84	32660	76.94	23.06	68.26	52.73
	19-771 122 NASH	15.49	257.37	28.41	110396	82.45	17.55	82.90	183.43
	19-771 123 NASH	13.64	247.69	22.68	91578	75.80	24.20	65.09	166.29
	19-771 124 NASH	16.41	307.54	22.24	72313	80.82	19.18	76.89	135.51
	19-771 125 NASH	14.71	283.59	21.11	74451	79.09	20.91	72.70	143.53
	19-771 146 NASH	11.99	204.53	17.78	86924	75.70	24.30	64.61	148.31
	19-771 147 NASH	15.53	276.91	23.02	83150	77.12	22.88	68.86	148.22
	19-771 148 NASH	15.88	259.41	23.76	91583	83.35	16.65	89.03	149.59
	19-771 149 NASH	15.94	302.20	25.73	85143	80.98	19.02	80.15	161.42
19-771 150 NASH	16.98	289.45	25.42	87834	83.79	16.21	91.21	149.70	

* Micro droplet < 65 um²

* Macro droplet > 65 um²

Table 2. Steatosis Analysis Summary 39-Weeks (After Efficacy Study Conclusion)

Data for the 39-week timepoint with the control (standard NIH-31M diet), the NASH diet conditioned vehicle group (NASH diet), the Elafibranor-treated NASH, and OCA-treated NASH groups showing total lipid area as well as more granular lipid data such as amount and type for individual hepatocytes.

Treatment	Sample	% Lipid Area	Mean Lipid per Hepatocyte (um ²)	Total Lipid Area (mm ²)	Total Number of Hepatocytes	% Macrovesicular	% Microvesicular	Mean Vesicle Size (um ²)	Tissue Area Analyzed (mm ²)
NIH-31M Diet	19-684 205 GRP03	0.27	2.87	0.09	31258	10.64	89.36	24.31	33.09
	19-684 208 GRP03	0.20	2.09	0.06	30769	16.94	83.06	32.62	32.11
	19-684 212 GRP03	0.15	2.80	0.07	24547	13.49	86.51	18.97	46.79
	19-684 213 GRP03	0.20	3.93	0.06	14976	8.29	91.71	14.40	29.03
	19-684 217 GRP03	0.21	3.33	0.03	9016	17.90	82.10	25.52	14.20
NASH Diet	19-684 118 GRP04	12.68	223.10	5.22	23402	81.95	18.05	83.01	41.17
	19-684 175 GRP04	13.59	206.69	5.28	25547	82.78	17.22	89.54	38.86
	19-684 194 GRP04	12.90	197.17	6.43	32607	81.76	18.24	86.90	49.82
	19-684 197 GRP04	12.85	206.51	4.16	20121	84.14	15.86	94.28	32.34
Elafibranor	19-684 200 GRP04	13.91	227.35	5.03	22139	84.05	15.95	95.85	36.19
	19-684 127 GRP05	3.14	52.12	1.53	29395	87.16	12.84	106.38	48.74
	19-684 143 GRP05	2.70	35.14	1.11	31634	82.00	18.00	83.45	41.17
	19-684 159 GRP05	2.95	46.32	1.19	25693	83.17	16.83	89.09	40.41
OCA	19-684 167 GRP05	2.86	42.67	1.28	30080	88.17	11.83	108.94	44.91
	19-684 169 GRP05	4.04	51.12	1.67	32573	83.42	16.58	89.02	41.17
	19-684 104 GRP06	3.88	41.65	0.93	22237	76.94	23.06	70.58	23.87
	19-684 105 GRP06	5.45	72.08	1.53	21240	74.14	25.86	65.94	28.10
	19-684 176 GRP06	7.91	94.23	7.36	78083	81.86	18.14	82.26	93.03
OCA	19-684 177 GRP06	10.16	119.20	6.19	51956	80.21	19.79	76.93	60.94
	19-684 180 GRP06	5.46	65.48	5.12	78262	65.17	34.83	48.69	93.79

* Micro droplet < 65 um²

* Macro droplet > 65 um²

Table 3. Ballooning Analysis Summary 30-Weeks (Baseline)

Data for the 30-week timepoint with the control (standard NIH-31M diet) and the NASH diet conditioned group (NASH diet) showing the density of ballooning hepatocytes, the tissue area analyzed (mm²) and the presence or absence of Mallory-Denk bodies.

Treatment	Sample	Ballooning Hepatocyte Density (cells/cm ²)	Tissue Area Analyzed (mm ²)	Mallory Bodies- Present or Absent
NIH-31M Diet	19-771 201 STND	0.00	103.24	Absent
	19-771 202 STND	0.00	74.16	Absent
	19-771 204 STND	0.00	84.86	Absent
	19-771 214 STND	0.00	120.29	Absent
	19-771 215 STND	0.00	89.64	Present
NASH Diet	19-771 121 NASH	13.27	52.73	Present
	19-771 122 NASH	17.99	183.43	Present
	19-771 123 NASH	37.29	166.29	Present
	19-771 124 NASH	20.66	135.51	Present
	19-771 125 NASH	11.84	143.53	Present
	19-771 146 NASH	13.48	148.31	Present
	19-771 147 NASH	16.19	148.22	Present
	19-771 148 NASH	19.39	149.59	Present
	19-771 149 NASH	25.40	161.42	Present
19-771 150 NASH	12.69	149.70	Present	

Table 4. Ballooning Analysis Summary 39-Weeks (After Efficacy Study Conclusion)

Data for the 39-week timepoint with the control (standard NIH-31M diet), the NASH diet conditioned vehicle group (NASH diet), the Elafibranor-treated NASH, and OCA-treated NASH groups showing the density of ballooning hepatocytes, the tissue area analyzed (mm²) and the presence or absence of Mallory-Denk bodies.

Treatment	Sample	Ballooning Hepatocyte Density (cells/cm ²)	Tissue Area Analyzed (mm ²)	Mallory Bodies- Present or Absent
NIH-31M Diet	19-684 205 GRP03	0.00	33.09	Absent
	19-684 208 GRP03	0.00	32.11	Absent
	19-684 212 GRP03	0.00	46.79	Absent
	19-684 213 GRP03	0.00	29.03	Absent
	19-684 217 GRP03	0.00	14.20	Absent
NASH Diet	19-684 118 GRP04	92.31	41.17	Present
	19-684 175 GRP04	74.62	38.86	Present
	19-684 194 GRP04	40.14	49.82	Present
	19-684 197 GRP04	46.38	32.34	Present
	19-684 200 GRP04	33.16	36.19	Present
Elafibranor	19-684 127 GRP05	0.00	48.74	Absent
	19-684 143 GRP05	19.43	41.17	Present
	19-684 159 GRP05	2.47	40.41	Present
	19-684 167 GRP05	6.68	44.91	Present
	19-684 169 GRP05	12.14	41.17	Present
OCA	19-684 104 GRP06	16.75	23.87	Present
	19-684 105 GRP06	35.59	28.10	Present
	19-684 176 GRP06	13.97	93.03	Present
	19-684 177 GRP06	9.85	60.94	Present
	19-684 180 GRP06	18.13	93.79	Present

Table 5. Inflammatory Cell Analysis Summary 30-Weeks (Baseline)

Data for the 30-week timepoint with the control (standard NIH-31M diet) and the NASH diet conditioned group (NASH diet) showing the density of immune cells, the total number and area of immune cells, and the tissue area analyzed (mm²).

Treatment	Sample	Immune Cell Density (cells/mm ²)	Total Immune Cell Area (mm ²)	Immune Cell Count	Tissue Area Analyzed (mm ²)
NIH-31M Diet	19-771 201 STND	212.15	3.15	21902	103.24
	19-771 202 STND	194.75	2.08	14443	74.16
	19-771 204 STND	234.14	2.63	19869	84.86
	19-771 214 STND	113.91	1.96	13703	120.29
	19-771 215 STND	159.19	2.08	14270	89.64
NASH Diet	19-771 121 NASH	292.51	1.94	15425	52.73
	19-771 122 NASH	301.32	6.93	55270	183.43
	19-771 123 NASH	229.57	4.87	38174	166.29
	19-771 124 NASH	218.60	3.93	29624	135.51
	19-771 125 NASH	266.22	4.82	38210	143.53
	19-771 146 NASH	266.23	4.89	39485	148.31
	19-771 147 NASH	197.98	3.78	29345	148.22
	19-771 148 NASH	245.14	4.56	36670	149.59
	19-771 149 NASH	163.49	3.48	26391	161.42
19-771 150 NASH	189.28	3.51	28335	149.70	

Table 6. Inflammatory Cell Analysis Summary 39-Weeks (After Efficacy Study Conclusion)

Data for the 39-week timepoint with the control (standard NIH-31M diet), the NASH diet conditioned vehicle group (NASH diet), the Elafibranor-treated NASH, and OCA-treated NASH groups showing the density of immune cells, the total number and area of immune cells, and the tissue area analyzed (mm²).

Treatment	Sample	Immune Cell Density (cells/mm ²)	Total Immune Cell Area (mm ²)	Immune Cell Count	Tissue Area Analyzed (mm ²)
NIH-31M Diet	19-684 205 GRP03	389.66	12892.00	1.93	33.09
	19-684 208 GRP03	313.72	10075.00	1.67	32.11
	19-684 212 GRP03	425.94	19928.00	2.37	46.79
	19-684 213 GRP03	365.21	10603.00	1.48	29.03
	19-684 217 GRP03	487.46	6921.00	0.89	14.20
NASH Diet	19-684 118 GRP04	580.28	23888.00	2.69	41.17
	19-684 175 GRP04	552.07	21456.00	2.26	38.86
	19-684 194 GRP04	626.62	31220.00	3.45	49.82
	19-684 197 GRP04	758.87	24545.00	2.69	32.34
	19-684 200 GRP04	571.04	20667.00	2.42	36.19
Elafibranor	19-684 127 GRP05	349.50	17036.00	1.52	48.74
	19-684 143 GRP05	675.25	27801.00	2.89	41.17
	19-684 159 GRP05	431.43	17434.00	1.72	40.41
	19-684 167 GRP05	613.49	27551.00	2.81	44.91
	19-684 169 GRP05	474.25	19526.00	1.89	41.17
OCA	19-684 104 GRP06	454.81	10858.00	1.4	23.87
	19-684 105 GRP06	449.76	12636.00	1.66	28.10
	19-684 176 GRP06	482.61	44899.00	5.64	93.03
	19-684 177 GRP06	550.19	33527.00	4.09	60.94
	19-684 180 GRP06	516.70	48461.00	5.67	93.79

Table 7. Fibrosis Analysis Summary (PSR) 30-Weeks (Baseline)

Data for the 30-week timepoint with the control (standard NIH-31M diet) and the NASH diet conditioned group (NASH diet) showing the percent fibrosis area (%), the area of total fibrosis (mm²), and the tissue area analyzed (mm²).

Treatment	Sample	Percent Fibrosis Area (%)	Total Fibrosis Area (mm ²)	Tissue Area Analyzed (mm ²)
NIH-31M Diet	19-771 201 STND	2.58	2.77	107.48
	19-771 202 STND	3.50	2.68	76.48
	19-771 204 STND	0.49	0.48	96.96
	19-771 214 STND	3.33	4.02	120.47
	19-771 215 STND	3.05	2.70	88.53
NASH Diet	19-771 121 NASH	7.71	4.02	52.21
	19-771 122 NASH	9.15	16.27	177.82
	19-771 123 NASH	10.60	17.76	167.54
	19-771 124 NASH	6.99	9.47	135.63
	19-771 125 NASH	9.55	13.72	143.67
	19-771 146 NASH	12.01	17.80	148.29
	19-771 147 NASH	9.40	14.46	153.82
	19-771 148 NASH	10.54	15.64	148.38
	19-771 149 NASH	6.57	10.56	160.73
19-771 150 NASH	10.47	15.55	148.62	

Table 8. Fibrosis Analysis Summary (PSR) 39-Weeks (After Efficacy Study Conclusion)

Data for the 39-week timepoint with the control (standard NIH-31M diet), the diet conditioned vehicle group (NASH diet), the Elafibranor-treated NASH, and OCA-treated NASH groups showing the percent fibrosis area (%), the area of total fibrosis (mm²), and the tissue area analyzed (mm²).

Treatment	Sample	Percent Fibrosis Area (%)	Total Fibrosis Area (mm ²)	Tissue Area Analyzed (mm ²)
NIH-31M Diet	19-684 205 GRP03	1.55	0.49	31.89
	19-684 208 GRP03	1.35	0.43	31.74
	19-684 212 GRP03	1.55	0.70	45.05
	19-684 213 GRP03	1.14	0.30	26.11
	19-684 217 GRP03	0.33	0.04	13.25
NASH Diet	19-684 118 GRP04	3.57	1.34	37.35
	19-684 175 GRP04	4.77	1.82	38.15
	19-684 194 GRP04	5.16	2.26	43.83
	19-684 197 GRP04	8.32	2.37	28.50
	19-684 200 GRP04	4.72	1.60	33.84
Elafibranor	19-684 127 GRP05	1.70	0.68	39.91
	19-684 143 GRP05	3.91	1.40	35.89
	19-684 159 GRP05	2.83	0.92	32.38
	19-684 167 GRP05	2.96	1.08	36.50
	19-684 169 GRP05	3.10	1.35	43.46
OCA	19-684 104 GRP06	4.41	0.94	21.23
	19-684 105 GRP06	5.50	1.29	23.48
	19-684 176 GRP06	1.64	1.65	100.66
	19-684 177 GRP06	1.67	1.38	82.89
	19-684 180 GRP06	4.51	3.90	86.46

REFERENCES

Kleiner DE, Brunt EM, Van Natta M, Behling C, Contos MJ, Cummings OW, Ferrell LD, Liu YC, Torbenson MS, Unalp-Arida A, Yeh M, McCullough AJ, Sanyal AJ; Nonalcoholic Steatohepatitis Clinical Research Network. Design and validation of a histological scoring system for nonalcoholic fatty liver disease. *Hepatology*. 2005 Jun;41(6):1313-21.

Kleiner DE, Makhlof HR. Histology of Nonalcoholic Fatty Liver Disease and Nonalcoholic Steatohepatitis in Adults and Children. *Clin Liver Dis*. 2016 May;20(2):293-312.

Bedossa P and the FLIP Pathology Consortium. Fatty liver inhibition of progression (FLIP) algorithm and steatosis, activity, and fibrosis (SAF) score in the evaluation of biopsies of nonalcoholic fatty liver disease. *Hepatology*. 2014 Apr;60(2):565-575.

Kleiner DE, Brunt EM, Wilson LA, Behling C, Guy C, Contos M, Cummings O, Yeh M, Gill R, Chalasani N, Neushwander-Tetri BA, Diehl AM, Dasarathy S, Terrault N, Kowdley K, Loomba R, Belt P, Lavine JE, Sanyal AJ. Association of histologic disease activity with progression of nonalcoholic fatty liver disease. *Gastroenterology and Hepatology*. 2019 Oct;2(10):1-16.

Makri E, Cholangitas E, Tziomalos K. Emerging role of obeticholic acid in the management of nonalcoholic fatty liver disease. *World Journal of Gastroenterology*. 2016 Nov;22(41):9039-43.

Pai RK, Kleiner DE et al. *Aliment Pharmacol Ther*. Standardizing the interpretation of liver biopsies in non-alcoholic fatty liver disease clinical trials. 2019 Nov;50(10):1100-1111.

Ratziu V, Harrison SA, Francque S, Bedossa P, Lehert P, Serfaty L, Romero-Gomez M, Boursier J, Abdelmalek M, Caldwell S, Drenth J, Anstee QM, Hum D, Hanf R, Roudot A, Megnier S, Staels B, Sanyal A. Elafibranor, an Agonist of the peroxisome proliferator-activated receptor- α and $-\delta$, induces resolution of nonalcoholic steatohepatitis without fibrosis worsening. 2016 May;150 (5):1147-1159.